Magnetoresistance of semimetals: The case of antimony

Benoît Fauqué,[1,2,*] Xiaojun Yang,[2,3] Wojciech Tabis,[4,5] Mingsong Shen,[6] Zengwei Zhu,[6] Cyril Proust,[4]
Yuki Fuseya,[2,7] and Kamran Behnia[2,†]

[1]*JEIP, USR 3573 CNRS, Collège de France, PSL Research University, 11, place Marcelin Berthelot, 75231 Paris Cedex 05, France*
[2]*ESPCI ParisTech, PSL Research University CNRS, Sorbonne Universités, UPMC Univ. Paris 6, LPEM,
10 rue Vauquelin, F-75231 Paris Cedex 5, France*
[3]*School of Physics and Optoelectronics, Xiangtan University, Xiangtan 411105, China*
[4]*Laboratoire National des Champs Magnétiques Intenses (LNCMI-EMFL), CNRS, UGA, UPS, INSA, Grenoble/Toulouse, France*
[5]*AGH University of Science and Technology, Faculty of Physics and Applied Computer Science, 30-059 Krakow, Poland*
[6]*Wuhan National High Magnetic Field Center and School of Physics, Huazhong University of Science and Technology, Wuhan 430074, China*
[7]*Department of Engineering Science, University of Electro-Communications, Chofu, Tokyo 182-8585, Japan*

Large unsaturated magnetoresistance has been recently reported in numerous semimetals. Many of them have a topologically nontrivial band dispersion, such as Weyl nodes or lines. Here, we show that elemental antimony displays the largest high-field magnetoresistance among all known semimetals. We present a detailed study of the angle-dependent magnetoresistance and use a semiclassical framework invoking an anisotropic mobility tensor to fit the data. A slight deviation from perfect compensation and a modest variation with magnetic field of the components of the mobility tensor are required to attain perfect fits at arbitrary strength and orientation of magnetic field in the entire temperature window of study. Our results demonstrate that large orbital magnetoresistance is an unavoidable consequence of low carrier concentration and the subquadratic magnetoresistance seen in many semimetals can be attributed to field-dependent mobility, expected whenever the disorder length scale exceeds the Fermi wavelength.

I. INTRODUCTION

Detailed studies of magnetoresistance have been carried out in a large variety of systems ranging from ferromagnetic-metallic multilayer devices [1], manganite perovskites [2], and doped semiconductors [3]. The large increase in the resistivity of semimetals, which appears when the magnetic field is applied perpendicular to the orientation of the electric current, has been known for a long time [4]. Recently, such a large orbital magnetoresistance has been observed in many dilute metals. The list includes three-dimensional Dirac systems (Cd_3As_2 [5]), Weyl semimetals (WTe_2 [6], NbP [7] or WP_2 [8,9], LaBi [10]), but also 'trivial' semimetals (LaSb [11], gray arsenic [12]). Reporting on the large magnetoresistance in WTe_2, Ali *et al.* [6] contrasted its unsaturated B^2 behavior to the quasilinear and eventually saturating high-field magnetoresistance of well-known semimetals such as bismuth and graphite. Soon afterwards, WTe_2 was identified as a type-II Weyl semimetal [13]. During the last three years, the link between amplitude and the field dependence of magnetoresistance and its possible link to nontrivial electronic topology became a subject of debate and motivated numerous studies.

Here, we present the case of elemental antimony, a semimetal with high mobility carriers [14,15] and topologically nontrivial surface states [16]. Its large magnetoresistance, reported by Brandt and collaborators [17] decades ago, has escaped the attention of the community exploring high-field large unsaturated magnetoresistance (see, i.e., Refs. [5–12,18–21]). It is true that [17] did not scrutinize the amplitude of the magnetoresistance, the subject of the present letter, comparing Sb with other, topological or trivial, semimetals. The carrier density of Sb is $n \simeq p \simeq 5.5 \times 10^{19}$ cm^{-3} [23]; it is comparable to WTe_2 ($n \simeq p \simeq 6.6 \times 10^{19}$ cm^{-3} [22]) and two orders of magnitude larger than bismuth ($n \simeq p \simeq 3 \times 10^{17}$ cm^{-3} [24]). We show that in a reasonably clean Sb single crystal, a magnetic field of 56 T enhances resistivity by a factor of $\frac{\Delta \rho}{\rho_0} = 3 \times 10^6$. This is one order of magnitude higher than what was reported in WTe_2 [6] and comparable with what was observed in WP_2 [8]. The field dependence of magnetoresistance is close to (but slightly different from) quadratic. We present an angle-dependent study, with magnetic field kept perpendicular to the applied current and rotating in three perpendicular crystalline planes (as in the case of bismuth [25]), and employ a semiclassical picture, based on distinct mobility tensors for electrons and holes, to explain the data. We show that by assuming slightly imperfect compensation, one can explain the finite Hall response. Taking into account a smooth field-induced reduction in mobility allows perfect fits to the nonquadratic magnetoresistance and the nonlinear Hall resistivity at the same time. Thus, antimony becomes the first semimetal whose extremely large magnetoresistance is totally explained by an extended semiclassical treatment for any arbitrary amplitude and orientation of magnetic field.

---
*benoit.fauque@espci.fr
†kamran.behnia@espci.fr

The two additional assumptions required to attain perfect fits bring new insight to the apparent diversity of semimetallic magnetoresistance. Imperfect compensation caused by 1 part per million (ppm) of uncontrolled doping is barely noticeable when there is one hole and one electron per 10^4 atoms, that is when carrier density is in the range of 10^{19} cm^{-3}. But the same amount of uncontrolled doping has a much stronger signature when the carrier density is two orders of magnitude lower. This explains why the high-field magnetoresistance is close to quadratic in Sb and WTe$_2$ but almost linear in Bi. The field-induced reduction in mobility can be caused by a disorder invisible to long-wavelength electrons at zero field and becomes relevant in the presence of magnetic field. Electrons with a long wavelength are not efficiently scattered by neutral or charged defects of atomic size. However, with increasing magnetic field, a subset of spatially-extended defects smaller than the Fermi wavelength become relevant as scattering centers, because they can interact with electrons with small momentum along the magnetic field [26]. This provides a simple but nonuniversal foundation for the field-induced decrease in mobility leading to the ubiquitous nonquadratic magnetoresistance.

II. RESULTS

Figure 1(a) presents the reported magnetoresistance of numerous semimetals at $B = 9$ T and $T = 2$ K extracted from Refs. [7,8,11,12,18,19,21,22,27–33] (see Ref. [34] for details). The amplitude of field-induced enhancement in resistivity is plotted as a function of zero-field mobility, extracted from resistivity and carrier density: $\mu_0 = \frac{1}{\rho_0(n+p)e}$. Here, e is the charge of the electron, n and p are the electron and hole densities, and ρ_0 the zero-field resistivity at $T = 2$ K. One can see that across more than three orders of magnitude, the MR of semimetals (topological or not) roughly scales with their zero-field mobility. The higher the mobility, the larger the magnetoresistance. However, one can also see that systematically $\frac{\Delta\rho}{\rho_0}$ is lower than $81\langle\mu_0^2\rangle$, which is what is expected for 9 T if the mobility was the same unique number relevant to the two [zero-field conductivity, $\sigma = e(n\mu_e + p\mu_h)$, and finite-field magnetoresistance].

Even the most ideally simple semimetal requires more complexity. Such a system would have a single electronlike and a single holelike Fermi surface. The two pockets are isotropic with scalar mobilities of μ_e and μ_h. The semiclassic magnetoresistance of such a system would be $\frac{\Delta\rho}{\rho_0} = \langle\mu_m^2\rangle B^2$, where $\mu_m = \sqrt{\mu_e\mu_h}$. Note that the zero-field average mobility is $\mu_0 = \frac{n\mu_e + p\mu_h}{(n+p)}$. The two average mobilities are identical only when $n = p$ and $\mu_e = \mu_h$. However, μ_0 and μ_m remain of the same order of magnitude.

As seen in Fig. 1(a), despite the discovery of numerous new compounds, the three elemental semimetals (Bi, Sb, and As) are still those showing the largest magnetoresistance at 9 T. Figure 1(b) compares the field dependence of magnetoresistance in bismuth, WTe$_2$, and antimony at $T = 2$ K and $B \leqslant 56$ T. One can see that it is close to B^2 in Sb and WTe$_2$ but presents a lower exponent (B$^{1.5}$) and a tendency to saturation in bismuth. As a consequence, antimony surpasses bismuth above ≈ 25 T. Note that the amplitude of magnetoresistance in
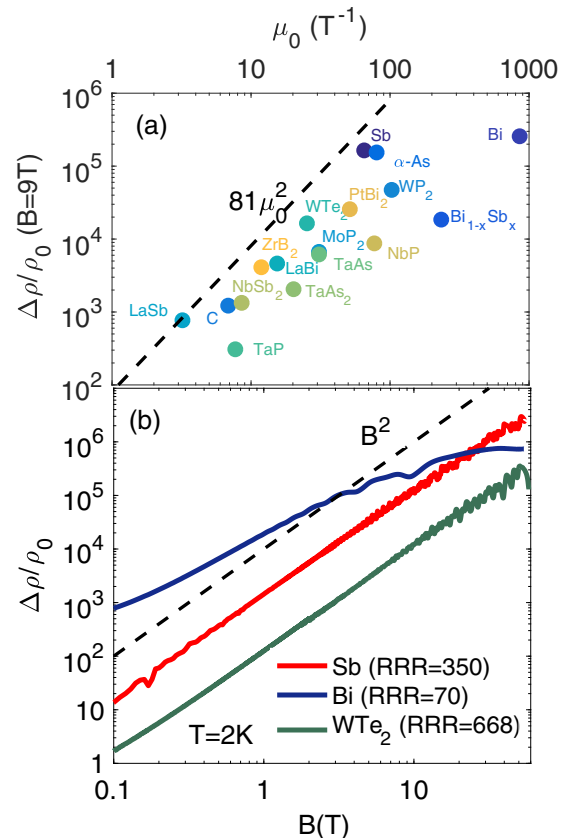

FIG. 1. (a) Magnetoresistance of various semimetals at $B = 9$ T and $T = 2$ K as a function of the mobility $\mu_0 = \frac{1}{\rho_0(n+p)e}$ where e is the charge of the electron, n and p are the electron and hole density, and ρ_0 the zero field resistivity at 2 K. μ_0 is expressed in Tesla^{-1} = 10^4 cm^2 V^{-1} s^{-1}. The points are extracted from the references [7,8,11,12,18,19,21,22,27–33] (see Ref. [34] for details). (b) Magnetoresistance of elemental semimetals antimony (j//trigonal and B//bisectrix), bismuth (j//bisectrix and B//trigonal) and WTe$_2$ (j//a axis and B//c axis) at $T = 2$ K. RRR (residual resistivity ratio) is equal to $\frac{\rho(T=300 \text{ K})}{\rho(2 \text{ K})}$.

a given metal is not fixed and depends on the cleanness as we will discuss below.

A more elaborate picture requires one to consider the tensorial nature of mobility. We attempted to achieve this by studying the angle dependence of ρ_{ii} in Sb when the magnetic field rotates in the plane perpendicular to the i axis. Here, ($i = 1,2,3$) refer to the binary, bisectrix, and trigonal crystal axes. The three planes of rotations are P$_1$ = (trigonal, bisectrix), P$_2$ = (trigonal, binary), and P$_3$ = (binary, bisectrix), as in the case of bismuth [25].

The Fermi surface of Sb has been intensively studied by quantum oscillations [17,23] and cyclotron resonance [35]. These studies have found that the density of electron and hole pockets is equal to $n = p = 5.5 \times 10^{19}$ cm^{-3}, within a precision of 1% [23]. In these studies, the Fermi surface was taken to be three equivalent electron pockets and six equivalent hole pockets. The electron pockets are quasiellipsoids centered at the L points of the Brillouin zone and reminiscent of the case of bismuth. The hole pockets consist of two groups of three pockets slightly off the T points of the Brillouin zone and
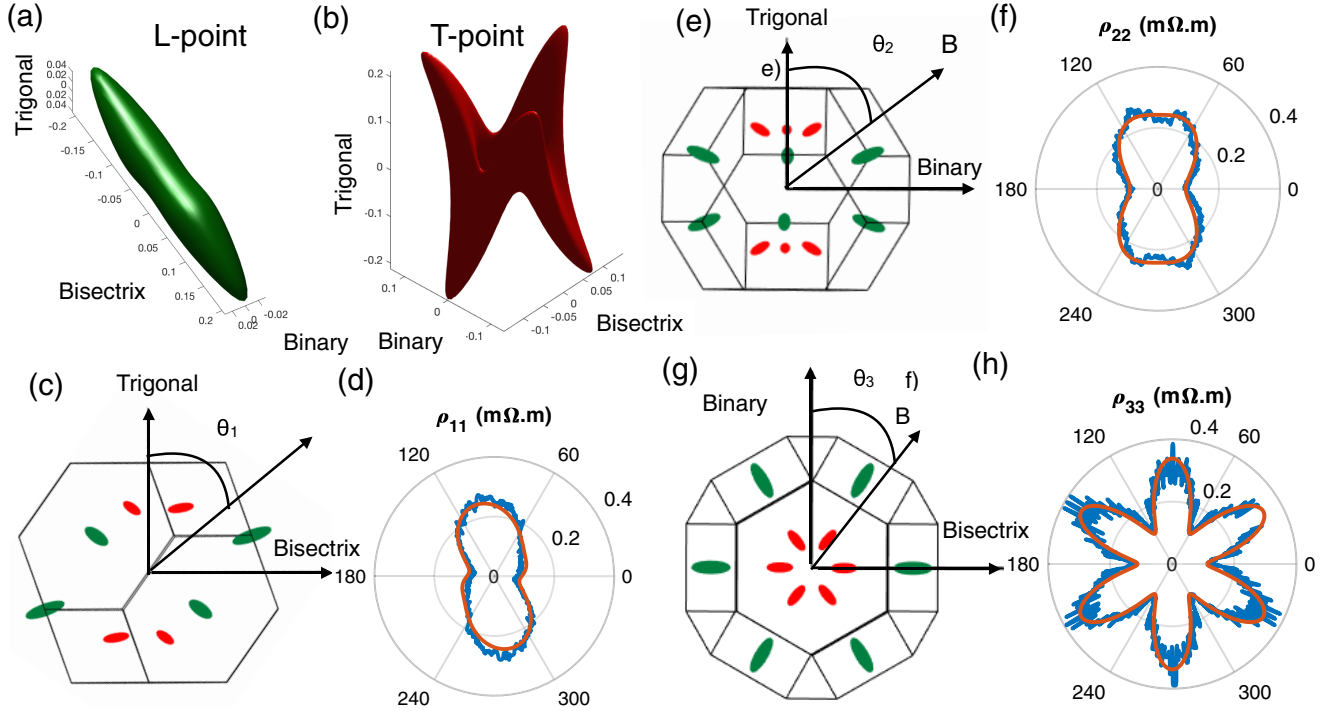
FIG. 2. Angular dependence of the magnetoresistance of antimony. (a),(b) Electron and hole Fermi surface of antimony according to the Liu and Allen tight-binding model. The unit of reciprocal length is $g = 1.461$ Å^{-1}. (c),(e),(g) Sketch of the Brillouin zone and the Fermi surface of antimony projected in the three planes of rotation P$_1$ (trigonal, bisectrix), P$_2$ (trigonal, binary), and P$_3$ (binary, bisectrix). (d),(f),(h) ρ_{ii} for $i = 1$, 2, and 3 in the three planes of rotation P$_1$, P$_2$, and P$_3$ in blue at $T = 2$ K and $B = 12$ T (the electric current is applied along the crystal axis perpendicular to the rotating plane) measured on the same sample. The red line is a fit using a theoretical model described in the text.

therefore nonisomorphic to the case of bismuth. According to the tight-binding model used by Liu and Allen [24], as discussed in the Supplemental Material Sec. C [34], the six hole pockets are interconnected around the T point, as shown in Fig. 2(b), a feature not explicitly mentioned previously [24].

The angle dependence of the magnetoresistance at $T = 2$ K and $B = 12$ T measured on the same sample for the three perpendicular planes of field rotation are presented in Figs. 2(d), 2(f) and 2(h). In each case, the profile of $\rho_{ii}(\theta)$ reflects the symmetry of the projected profile of the Fermi surface components in that plane [Figs. 2(c), 2(e) and 2(g)]. When the current is along the binary and the magnetic field rotates in the P$_1$ plane, there is only the inversion symmetry so that: $\rho_{11}(\theta) = \rho_{11}(\pi + \theta)$. When the current is along the bisectrix and a magnetic field rotates in the P$_2$ plane, as a consequence of additional mirror symmetry, $\rho_{22}(\theta) = \rho_{22}(-\theta)$. Finally, when the current is along the trigonal and the field rotates in the P$_3$ plane, sixfold oscillations result as a consequence of the C$_3$ symmetry combined with the inversion symmetry. In contrast to bismuth [25,36] we did not observe any field-induced loss of threefold symmetry (see Sec. E of Ref. [34] for more details).

III. DISCUSSION

A. The Mackey and Sybert formalism

In order to extract the components of the mobility tensor for electrons and holes, we used the formalism developed first by Mackey and Sybert [37] and then by Aubrey [38]. In this approach, the total conductivity is the sum of the contributions by each valley expressed as:

$$\hat{\sigma}_{e,h} = ne \left(\hat{\mu}_{e,h}^{-1} \mp \hat{B} \right)^{-1}, \tag{1}$$

where $\hat{B}$ is defined as:

$$\hat{B} = \begin{pmatrix} 0 & -B_3 & B_2 \\ B_3 & 0 & -B_1 \\ -B_2 & B_1 & 0 \end{pmatrix}. \tag{2}$$

Here, $\hat{\mu}_{e,h}$ is the mobility tensor of electrons and holes. B$_1$, B$_2$, and B$_3$ are the projections of the magnetic field vector along the three principal axes. By employing this formalism, we could extract the components of the mobility tensor along the principal axes of the representative ellipsoids for electrons, μ_i, and holes, $\nu_i (i = 1, 2, 3)$. Further details can be found in Ref. [34] Sec. D.

Our best simultaneous fits of ρ_{11}, ρ_{22}, and ρ_{33} at $T = 2$ K and $B = 12$ T are represented in red in Fig. 2. We report on Fig. 4 and in Sec. D of Ref. [34] similar fits for different temperature and magnetic fields to obtain the magnitude of the components of the mobility tensors at any magnetic field and temperature in Fig. 5.

One can see that the temperature dependence closely tracks the temperature dependence of the zero-field mobility along
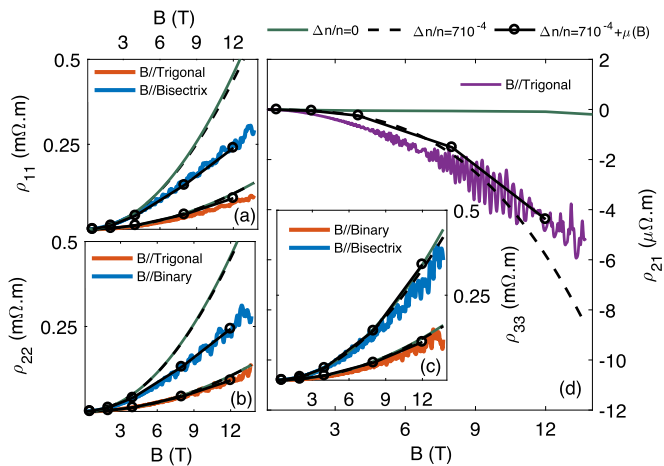
FIG. 3. Transverse magnetoresistance of Sb at $T = 2$ K along the axes of high symmetry: (a) $\rho_{11}(B)$ for B//trigonal (in blue) and B//bisectrix (in red), (b) $\rho_{22}(B)$ for B//trigonal (in blue) and B//binary (in red), (c) $\rho_{33}(B)$ for B//binary (in blue) and B//bisectrix (in red), (d) ρ_{12} for B//trigonal (in purple). The green lines correspond to the Mackey and Sybert's model assuming no change in mobility tensors with the magnetic field and a perfect compensation ($\frac{\Delta n}{n} = 0$). The dashed black lines correspond to the same model with a deviation from perfect compensation equal to $\frac{\Delta n}{n} = 7 \times 10^{-4}$ which allow us to capture the Hall response. The black lines correspond to the same model with a field dependence mobility tensor [reported in Fig. 4(b)] and a deviation from perfect compensation $\frac{\Delta n}{n} = 7 \times 10^{-4}$.

the trigonal axis: $\mu_0[\rho_{33}] = \frac{1}{ne\rho_{33}(B=0)}$. At low temperature, the components of the mobility tensor saturate. Above 10 K, they show a T^{-2}, like the one seen in bismuth [25] and attributed to intervalley carrier-carrier scattering [39]. The mobility tensors and the mass tensors are linked by $\hat{\mu}_{e,h} = e\hat{\alpha}_{e,h} \cdot \hat{\tau}_{e,h}$. Here, $\hat{\alpha}$ and $\hat{\tau}$ share the same principal axes and $\hat{\alpha}$ is the inverse of the mass tensor. Its components are the cyclotron masses [35]. The anisotropy of the scattering rate is set by (and is attenuated compared to) the anisotropy of the effective mass (see Sec. D of Ref. [34]). Let's discuss now the field dependance ρ_{11}, ρ_{22}, ρ_{33}, and ρ_{12}.

B. Deviation from compensation

In the Mackey-Sybert formalism, the Hall response is expected to be linear in the high-field regime ($\mu B \gg 1$) if the compensation is perfect. As illustrated in Fig. 3(d), experimentally, this is not the case. The nonlinear Hall resistivity can be captured by assuming a slight imbalance between hole and electron density, $\frac{\Delta n}{n} = \frac{p-n}{n}$. We find that the best agreement with data yields $\frac{\Delta n}{n} = 7 \times 10^{-4}$. This roughly corresponds to one defect per million unit cell, consistent with the 5 N quality Sb powder used to grow the sample and with early low magnetic field galvanometric measurements [15]. As illustrated in Figs. 3(a)–3(c), by including only the miscompensation (black dotted lines) ρ_{11}, ρ_{22}, ρ_{33} remain quadratic up to 14 T. On its own, the deviation from compensation is not responsible for the subquadratic behavior MR observed at low magnetic field and only affect it above 30 T as discussed in Ref. [27] section D.3.
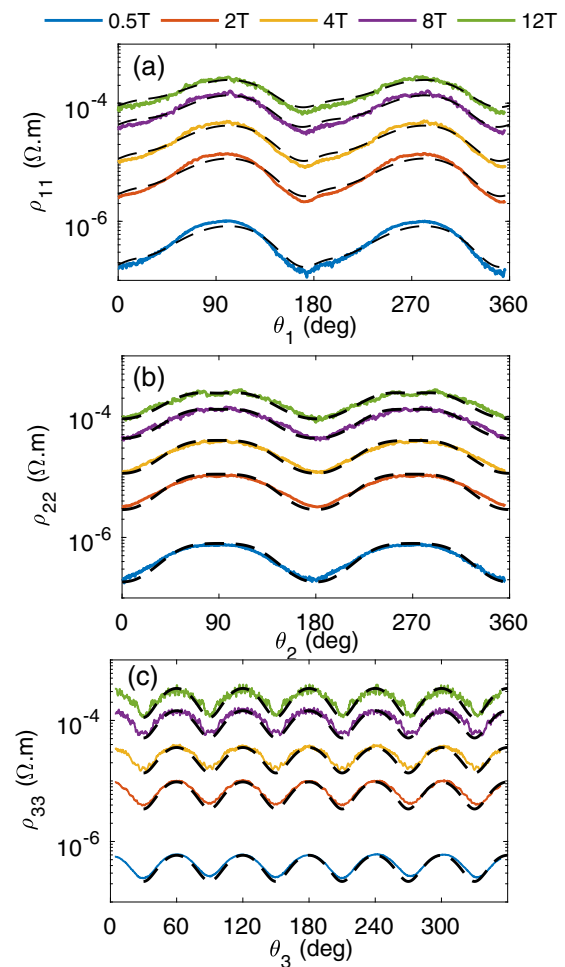

FIG. 4. Angular dependence of the magnetoresistance of Sb at $T = 2$ K for $B = 0.5$ T to 12 T in the three plans of rotations (a) P_1, (b) P_2, and (c) P_3. The dot lines are fits using the semiclassical model described in the text.

C. Field dependance mobility

A satisfactory description of the overall field dependence of ρ_{11}, ρ_{22}, ρ_{33}, and ρ_{12} is provided once we combine the imperfect compensation with a slight field dependence of the components of the mobility. When the field is swept from 0.5 T to 12 T, μ_1, ν_1, ν_2 are almost constant, but μ_2 and ν_3 decrease by a factor of 1.5 and μ_3 by a factor of 3. The fact that magnetic field does not affect in a similar manner among different components of the mobility tensor is a clue to the origin of the scattering process which becomes more effective in the presence of magnetic field. The drastic decrease in μ_3 indicates that disorder in the orientation perpendicular to the cleaving planes becomes more significant with increasing field. Another piece of evidence is provided by contrasting samples with different levels of disorder. As presented in Ref. [34], the subquadratic aspect of magnetoresistance becomes more pronounced in dirtier samples where both the RRR (residual resistivity ratio) and the Dingle mobility, μ_D are lower. A ratio of $\frac{\mu_0}{\mu_D}$ as large as 300 implies a significant role for small angle scattering. We thus conclude that the subquadratic MR of Sb is due to disorder characterized by a
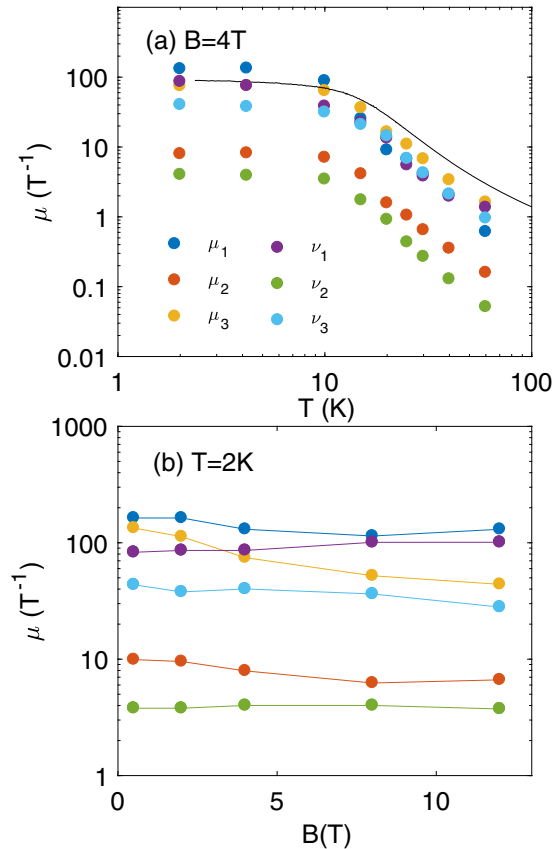
FIG. 5. Temperature and field dependence of mobility tensors of Sb: The hole and electron tensor component are, respectively, labeled (ν_1, ν_2, ν_3), (μ_1, μ_2, μ_3). (a) ν_i and μ_i for $i = 1, 2, 3$ at $B = 4$ T as a function of temperature. The black line is the mobility deduced from the temperature dependence of ρ_{33} in the Drude picture. (b) Field dependence of μ_i and ν_i for $i = 1, 2, 3$ at $T = 2$ K. The raw data and the comparison with the fit can be found in Ref. [34].

long range correlation scale. In the presence of both disorder and a magnetic field electrons with small momenta along the magnetic field can be trapped in the disorder potential. As the

magnetic field increases their electron motion is more and more confined into the minimum of the disorder potential leading to a decrease of the mean free path and thus of the mobility [26].

IV. CONCLUSION

In conclusion, we found a very large magnetoresistance in elemental antimony towering over most reported cases. We showed that the magnitude of the magnetoresistance at any temperature and magnitude or orientation of the magnetic field can be explained using a semiclassical framework with two additional ingredients, a weak deviation from perfect compensation and a field-dependent mobility tensor. The same framework can be used to address all other semimetals. We conclude that because of slight imperfect compensation subquadratic magnetoresistance is unavoidable. In antimony or in WTe$_2$, the carrier concentration is large enough to cover the role played by imperfect compensation, yet small enough to allow carriers to have a large mobility. This is the main reason behind its towering magnetoresistance. The phenomenological achievement reported here is only one step towards a microscopic theory. The challenge is to describe the anisotropic effect of magnetic field on carriers with a known dispersion in the presence of a precise scattering potential. This would pin down the intrinsic limits of mobility in a given material.

[1] P. M. Levy, Giant magnetoresistance in magnetic layered and granular materials, Solid State Phys. **47**, 367 (1994).

[2] C. N. R. Rao and B. Raveau (eds.), *Colossal Magnetoresistance Charge Ordering and Related Properties of Manganese Oxides* (World Scientific, Singapore, 1998).

[3] S. A. Solin, T. Thio, D. R. Hines, and J. J. Heremans, Enhanced room-temperature geometric magnetoresistance in inhomogeneous narrow-gap semiconductors, Science **289**, 1530 (2000).

[4] P. Kapitza, The study of the specific resistance of bismuth crystals and its change in strong magnetic fields and some allied problems, Proc. R. Soc. A **119**, 358 (1928).

[5] T. Liang, Q. Gibson, M. N. Ali, M. Liu, R. J. Cava, and N. P. Ong, Ultrahigh mobility and giant magnetoresistance in the Dirac semimetal Cd$_3$As$_2$, Nat. Mater. **14**, 280 (2015).

[6] M. N. Ali, J. Xiong, S. Flynn, J. Tao, Q. D. Gibson, L. M. Schoop, T. Liang, N. Haldolaarachchige, M. Hirschberger, N. P. Ong, and R. J. Cava, Large, non-saturating magnetoresistance in WTe$_2$, Nature (London) **514**, 205 (2014).

[7] C. Shekhar, A. K. Nayak, Y. Sun, M. Schmidt, M. Nicklas, I. Leermakers, U. Zeitler, Y. Skourski, J. Wosnitza, Z. Liu, Y. Chen, W. Schnelle, H. Borrmann, Y. Grin, C. Felser, and B. Yan, Extremely large magnetoresistance and ultrahigh mobility in the topological Weyl semimetal candidate NbP, Nat. Phys. **11**, 645 (2015).

[8] N. Kumar, Y. Sun, N. Xu, K. Manna, M. Yao, V. Süss, I. Leermakers, O. Young, T. Förster, M. Schmidt, H. Borrmann, B. Yan, U. Zeitler, M. Shi, C. Felser, and C. Shekhar, Extremely high magnetoresistance and conductivity in the type-II Weyl semimetals WP$_2$ and MoP$_2$, Nat. Commun. **8**, 1642 (2017).

[9] R. Schonemann, N. Aryal, Q. Zhou, Y.-C. Chiu, K.-W. Chen, T. J. Martin, G. T. McCandless, J. Y. Chan, E. Manousakis, and

L. Balicas, Fermi surface of the Weyl type-II metallic candidate WP$_2$, Phys. Rev. B **96**, 121108 (2017).

[10] S. Shanshan, W. Qi, G. Peng Jie, L. Kai, and L. Hechang, Large magnetoresistance in LaBi: origin of field-induced resistivity upturn and plateau in compensated semimetals, New J. Phys. **18**, 082002 (2016).

[11] F. F. Tafti, Q. D. Gibson, S. K. Kushwaha, N. Haldolaarachchige, and R. J. Cava, Consequences of breaking time reversal symmetry in LaSb: A resistivity plateau and extreme magnetoresistance, Nat. Phys. **12**, 272 (2016).

[12] L. Zhao, Q. Xu, X. Wang, J. He, J. Li, H. Yang, Y. Long, D. Chen, H. Liang, C. Li, M. Xue, J. Li, Z. Ren, L. Lu, H. Weng, Z. Fang, X. Dai, and G. Chen, Magnetotransport properties in a compensated semimetal gray arsenic, Phys. Rev. B **95**, 115119 (2017).

[13] A. A. Soluyanov, D. Gresch, Z. Wang, Q. Wu, M. Troyer, X. Dai, and B. A. Bernevig, Type-II Weyl semimetals, Nature (London) **527**, 495 (2015).

[14] B. N. Aleksansdrov, V. V. Dukin, L. A. Maslova, and S. V. Tsivinsk, Effect of size and temperature on the electric resistance of antimony single crystals, Zh. Eksp. Teor. Fiz. **61**, 243 (1971) [Sov. Phys. JETP **34**, 125 (1972)].

[15] M. S. Bresler and N. A. Red'ko, Galvanomagnetic phenomena in antimony at low temperatures, Zh. Eksp. Teor. Fiz. **61**, 287 (1971) [Sov. Phys. JETP **34**, 149 (1972)].

[16] J. Seo, P. Roushan, H. Beidenkopf, Y. S. Hor, R. J. Cava, and A. Yazdani, Transmission of topological surface states through surface barriers, Nature (London) **466**, 343 (2010).

[17] N. B. Brandt, E. A. Svistova, and T. V. Gorskaya, Electrical resistance of antimony in a magnetic field up to 420 kOe at liquid helium temperature, Zh. Eksp. Teor. Fiz. **53**, 1274 (1967) [Sov. Phys. JETP **26**, 745 (1968)].

[18] F. Arnold, C. Shekhar, S.-C. Wu, Y. Sun, R. D. dos Reis, N. Kumar, M. Naumann, M. O. Ajeesh, M. Schmidt, A. G. Grushin, J. H. Bardarson, M. Baenitz, D. Sokolov, H. Borrmann, M. Nicklas, C. Felser, E. Hassinger, and B. Yan, Negative magnetoresistance without well-defined chirality in the Weyl semimetal TaP, Nat. Commun. **7**, 11615 (2016).

[19] C.-L. Zhang, S.-Y. Xu, I. Belopolski, Z. Yuan, Z. Lin, B. Tong, G. Bian, N. Alidoust, C.-C. Lee, S.-M. Huang, T.-R. Chang, G. Chang, C.-H. Hsu, H.-T. Jeng, M. Neupane, D. S. Sanchez, H. Zheng, J. Wang, H. Lin, C. Zhang, H.-Z. Lu, S.-Q. Shen, T. Neupert, M. Z. Hasan, and S. Jia, Signatures of the Adler-Bell-Jackiw chiral anomaly in a Weyl fermion semimetal, Nat. Commun. **7**, 10735 (2016).

[20] Y. Luo, R. D. McDonald, P. F. S. Rosa, B. Scott, N. Wakeham, N. J. Ghimire, E. D. Bauer, J. D. Thompson, and F. Ronning, Anomalous electronic structure and magnetoresistance in TaAs$_2$, Sci. Rep. **6**, 27294 (2016).

[21] K. Wang, D. Graf, L. Li, L. Wang, and C. Petrovic, Anisotropic giant magnetoresistance in NbSb$_2$, Sci. Rep. **4**, 7328 (2014).

[22] Z. Zhu, X. Lin, J. Liu, B. Fauqué, Q. Tao, C. Yang, Y. Shi, and K. Behnia, Quantum Oscillations, Thermoelectric Coefficients,

and the Fermi Surface of Semimetallic WTe$_2$, Phys. Rev. Lett. **114**, 176601 (2015).

[23] L. R. Windmiller, de Haas-van Alphen effect and Fermi surface in antimony, Phys. Rev. **149**, 472 (1966).

[24] Y. Liu and R. E. Allen, Electronic structure of the semi-metals Bi and Sb, Phys. Rev. B **52**, 1566 (1995).

[25] A. Collaudin, B. Fauqué, Y. Fuseya, W. Kang, and K. Behnia, Angle Dependence of the Orbital Magnetoresistance in Bismuth, Phys. Rev. X **5**, 021022 (2015).

[26] J. C. W. Song, G. Refael, and P. A. Lee, Linear magnetoresistance in metals: Guiding center diffusion in a smooth random potential, Phys. Rev. B **92**, 180204(R) (2015).

[27] R. N. Bhargava, de Haas-van Alphen and galvanomagnetic effect in Bi and Bi-Pb alloys, Phys. Rev. **156**, 785 (1967).

[28] B. Fauqué, H. Yang, I. Sheikin, L. Balicas, J.-P. Issi, and K. Behnia, Hall plateaus at magic angles in bismuth beyond the quantum limit, Phys. Rev. B **79**, 245124 (2009).

[29] A. Banerjee, B. Fauqué, K. Izawa, A. Miyake, I. Sheikin, J. Flouquet, B. Lenoir, and K. Behnia, Transport anomalies across the quantum limit in semimetallic Bi$_{0.96}$Sb$_{0.04}$, Phys. Rev. B **78**, 161103(R) (2008).

[30] B. Fauqué, D. LeBoeuf, B. Vignolle, M. Nardone, C. Proust, and K. Behnia, Two Phase Transitions Induced by a Magnetic Field in Graphite, Phys. Rev. Lett. **110**, 266601 (2013).

[31] M. N. Ali, L. Schoop, J. Xiong, S. Flynn, Q. Gibson, M. Hirschberger, N. P. Ong, and R. J. Cava, Correlation of crystal quality and extreme magnetoresistance of WTe$_2$, Europhys. Lett. **110**, 67002 (2015).

[32] W. Gao, N. Hao, F-W. Zheng, W. Ning, M. Wu, X. Zhu, G. Zheng, J. Zhang, J. Lu, H. Zhang, C. Xi, J. Yang, H. Du, P. Zhang, Y. Zhang, and M. Tian, Extremely Large Magnetoresistance in a Topological Semimetal Candidate Pyrite PtBi$_2$, Phys. Rev. Lett. **118**, 256601 (2017).

[33] Q. Wang, P.-J. Guo, S. Sun, C. Li, K. Liu, Z.-Y. Lu, and H. Lei, Extremely large magnetoresistance and high-density Dirac-like fermions in ZrB$_2$, Phys. Rev. B **97**, 205105 (2018).

[34] See Supplemental Material at http://link.aps.org/supplemental/10.1103/PhysRevMaterials.2.114201 for the Fermi surface of Sb, a detailed discussion on the Mackey and Syber model and its application to Sb.

[35] W. R. Datars and J. Vanderkooy, Cyclotron resonance and the Fermi surface of antimony, IBM J. Res. Dev. **8**, 247 (1964).

[36] Z. Zhu, A. Collaudin, B. Fauqué, W. Kang and K. Behnia, Field-induced polarization of Dirac valleys in bismuth, Nat. Phys. **8**, 89 (2012).

[37] H. J. Mackey and J. R. Sybert, Magnetoconductivity of a Fermi ellipsoid with anisotropic relaxation time, Phys. Rev. **180**, 678 (1969).

[38] J. E. Aubrey, Magnetoconductivity tensor for semimetals, J. Phys. F **1**, 493 (1971).

[39] R. Hartman, Temperature dependence of the low-field galvanomagnetic coefficients of bismuth, Phys. Rev. **181**, 1070 (1969).